

# Degree One Loading by Pressure Variations at the CMB

Ming Fang, Bradford H Hager

*Department of Earth, Atmospheric & Planetary Sciences, Massachusetts Institute of Technology,  
Cambridge MA 02139, USA*

Weijia Kuang

*Planetary Geodynamics Laboratory, NASA Goddard Space Flight Center, USA*

**ABSTRACT:** Hemispherical asymmetry in core dynamics induces degree-1 pressure variations at the core mantle boundary (CMB), which in turn deforms the overlaying elastic mantle, at the same time keeps center of mass of the whole Earth stationary in space. We develop a systematic procedure to deal with the degree-1 CMB pressure loading. We find by direct calculation a surprisingly negative load Love number  $h_1 = -1.425$  for vertical displacement. Further analysis indicates that the negative  $h_1$  corresponds to thickening above the positive load that defies intuition that pressure inflation pushes overlaying material up and thins the enveloping shell. We also redefine the pressure load Love numbers in general to enable comparison between the surface mass load and the CMB pressure load for the whole spectrum of harmonic degrees. We find that the gravitational perturbations from the two kinds of loads at degrees  $n > 1$  are very similar in amplitude but opposite in sign. In particular, if the CMB pressure variation at degree 2 is at the level of  $\sim 1$  hpa/yr (1 cm water height per year), it would perturb the variation of Earth's oblateness, known as the  $J_2$ , at the observed level.

## INTRODUCTION

Advances in analyzing teleseismic waves and normal modes have shown evidences of Eastern-Western hemispherical asymmetry in material properties at the top of the Earth's inner core (e.g., Monnereau et al., 2010; Irving et al., 2009; Niu and Wen, 2001). There are two competing hypotheses in the attempt to explain this hemispherical asymmetry. The "lopsided growth" model (Monnereau et al., 2010)

---

This study was supported in part by NASA (No. NNX09AK 70G).

\*Corresponding author: fang@chandler.mit.edu

© China University of Geosciences and Springer-Verlag Berlin Heidelberg 2013

Manuscript received March 23, 2013.

Manuscript accepted June 2, 2013.

proposes an apparent translation caused by material crystallization in the Western Hemisphere of the inner core and, at the same time, melting in the Eastern Hemisphere. On the other hand, the "decentering" mechanism (Vamos and Suci, 2011) suggests that the spherically symmetrical inner core is simply off the geometric center towards the east in the equatorial plane by tens of kilometers. A third hypothesis relates to predicted models of solidification and melting of the inner core from CMB heat flux (Gubbins et al., 2011). Regardless of its details, the physical cause of the hemispherical symmetry of the inner core has to be consequentially in association with the dynamic processes in the fluid outer core and the mantle (e.g., Olson and Deguen, 2012; Buffet, 1996; Wahr and de Vries, 1989).

From geodetic prospective, hemispherical asymmetry in the Earth's interior can be viewed as a

background field, since its evolution is most likely in geological time scales. Observational evidences for tangible decadal variation in the core motion is associated with the flow at the upper reach of the outer core, which have been established based on the similarities between the decadal variation of the west drift of the magnetic field and the decadal variation of the Earth's rotation rate commonly known as variation in the length of day (Dumberry and Bloxham, 2004; Jackson et al., 1993). By "frozen flux" approximation (e.g., Roberts and Scott, 1965), the magnetic lines of force move along with the fluid parcels at the top reach of the outer core underneath the core mantle boundary (CMB). Thus, inversions for the core flow near the CMB and consequently geostrophic pressure variations underneath the CMB can be made from observations of the magnetic field (e.g., Fang et al., 1996; Gire and Le Mouél, 1990).

It is reasonable to assume that the magneto-hydrodynamic convection in the outer core dynamically decouples with the thermally driven convection in the mantle, because of the markedly different in characteristic time scales between the fluid core convection and the mantle convection (Kuang and Bloxham, 1997; Glatzmaier and Roberts, 1995). The dynamically decoupled mantle can be treated as an elastic shell, passively deforming in response to CMB pressure variations. Previous investigations on mantle deformation induced by CMB pressure loading (e.g., Greff and Le Mouél, 2004; Fang et al., 1996) have ignored the hemispherical asymmetry, i.e., the degree-1 component in spherical harmonic decomposition of the deformation field. One of the objectives of this work is to develop a new theory for degree-1 CMB pressure loading under the framework of the classical load Love numbers (Farrell, 1972; Longman, 1962).

The degree-1 loading in quasi-static elastic problems distinguishes itself by the rise, among all independent solutions, of a rigid shift that produces no strain and consequently makes the strain boundary conditions ill-conditioned. For surface mass loading, the degree-1 problem is solved originally by (Farrell, 1972), and later on perfected by Saito (1974) and Dahlen (1976). The key ingredient of the degree-1 solution is to impose additional constraint by specifying the reference frame of choice. As it turns out, the

degree-1 loading by the CMB pressure is not a simple extension of Farrell's solution (Farrell, 1972), because the core-mantle coupling is a process of internal adjustment of the Earth system, while in the surface loading problems the Earth as a whole adjusts the external loading. Interesting dynamic issues arise from the internal adjustments. In this article, we limit our discussions at the phenomenological level by presenting the generally physical consideration and mathematical procedure for treating the degree-1 loadings from the outer surface and from the CMB. In an earlier work (e.g., Fang et al., 1996) the Love numbers for the CMB loading for harmonic degrees  $n > 1$  are introduced in an ad hoc fashion. Here we streamline the general theory so that comparison could be made between the surface mass loading and the CMB pressure loading. This comparison allows us to further expose the peculiarity of the degree-1 loading by the CMB pressure.

As mentioned earlier, we treat the mantle as a self-gravitating, non-rotating, isotropic, and laterally homogeneous elastic shell specified by the PREM (Dziewonski and Anderson, 1981), which is passively deforming by the CMB pressure variation. In a separate investigation Dumberry and Bloxham (2004) argue that the CMB pressure variation not only perturbs the mantle but also perturbs the entire Earth including the core itself. This model in essence is to treat the applied CMB pressure variation as external sources completely foreign to the Earth. In our case, however, the CMB pressure variation arises from the motion of the core itself. Strictly speaking, motions in the mantle and the core are dynamically coupled. Our elastic shell model is a simplification of the coupled dynamic process. Validation of this simplification is shown in the APPENDIX. The key point is that if the entire core is dynamically adjusting to the prescribed CMB pressure variation, then an additional pressure perturbation will arise at the CMB due to the dynamic adjustment by the bulk of the fluid core. As a result, the total of the CMB pressure variation is no longer that prescribed at the CMB. But the "observed" CMB pressure by geostrophic inversion from the observed secular variation of the magnetic field can only be understood as the total of the CMB pressure variation (see APPENDIX) (e.g., Fang et al., 1996; Gire and Le

Mouël, 1990).

Technically, the terms spherical layer, spherical surface, or layer are always referred to being concentric with the outer surface of the Earth. The terms pressure or pressure anomaly always refer to the non-hydrostatic increments.

### GREEN FUNCTIONS FOR THE PRESSURE LOADS

We interchangeably use  $\Omega$  and colatitude-longitude  $(\theta, \varphi)$  for positions on the surface of a unit sphere in a geocentric frame. Specifically, we will choose the Combined Center of Mass of the Whole Earth (CCMWE), including the mantle and the core as our reference frame. For the purpose of comparability, we readdress the conventional surface mass load problem (Longman, 1962) as the mass-related surface pressure (MRSP) load, with the load mass described by an equivalent pressure. A pressure distribution over a layer of radius  $r$ , called an  $r$ -layer, is always projected onto the surface of a unit sphere, thus, a pressure distribution on the outer surface of radius  $a$  and on the CMB of radius  $b$  are both written as  $p(\Omega)$  or  $p(\theta, \varphi)$ . Surface displacement,  $\mathbf{u}$ , and gravitational perturbation,  $\Phi$ , due to an arbitrary pressure load,  $p(\Omega)$ , on an  $r$ -layer can be represented by Green functions  $(\mathbf{U}, \Phi)$

$$\begin{aligned} \mathbf{u}(a, \Omega) &= \int_{\Omega} \mathbf{U}(a, \Omega, \Omega') p(\Omega') r^2 d\Omega' \\ \Phi(a, \Omega) &= \int_{\Omega} \Phi(a, \Omega, \Omega') p(\Omega') r^2 d\Omega' \end{aligned} \quad (1)$$

The radius variable,  $r$ , in the left subscript of the Green functions specifies the  $r$ -layer of the pressure

$$\begin{aligned} \mathbf{U} &= \sum_{n=0}^{\infty} \sum_{m=-n}^n \left( \hat{\mathbf{r}} U_{nm}(r) Y_{nm}(\Omega) + V_{nm}(r) \left( \hat{\boldsymbol{\theta}} \frac{\partial}{\partial \theta} + \hat{\boldsymbol{\phi}} \frac{\partial}{\sin \theta \partial \varphi} \right) Y_{nm}(\Omega) \right) \\ \Phi &= \sum_{n=0}^{\infty} \sum_{m=-n}^n \Phi_{nm}(r) Y_{nm}(\Omega) \end{aligned} \quad (4)$$

where the un-normalized harmonics,  $Y_{nm}$ , are in the form

$$\begin{aligned} Y_{nm}(\theta, \varphi) &= P_n(\cos \theta) \sin m \varphi & m = 1, \dots, n \\ Y_{nm}(\theta, \varphi) &= P_n(\cos \theta) \cos m \varphi & m = -n, -(n-1), \dots, -1, 0 \end{aligned} \quad (5)$$

Note, the Earth model PREM is inverted from seismic data, and the frequency,  $\omega$ , of the fluctuation in the CMB pressure is very low compared to that of seismic normal modes, we follow the classic tidal

load, while the  $r^2$  term arises from the area element of the  $r$ -layer. It is understood that the Green function technique advocated by Longman (1962) is not necessary for load problems. Nonetheless, the method does have the advantage of clarity and historical continuity.

Denote by  $\mathbf{T}$  the stress tensor within the solid earth. The stress boundary condition for the Green functions on the  $r$ -layer of load is

$$\hat{\mathbf{r}} \cdot \mathbf{T}(r, \Omega, \Omega') = -\delta_r(\Omega, \Omega') \hat{\mathbf{r}} \quad (2)$$

where  $\hat{\mathbf{r}}$  is the unit radial vector and  $\delta_r$  the Dirac  $\delta$  function on the  $r$ -layer. The boundary condition (2) is valid for the outer surface load downward as well as for the internal pressure load upward, since the normal of an internal  $r$ -layer, as the boundary of the upper part of the mantle, is  $-\hat{\mathbf{r}}$ . The function  $\delta_r$  can be written in spherical harmonics

$$\begin{aligned} \delta_r(\Omega, \Omega') &= \frac{1}{4\pi r^2} \sum_{n=0}^{\infty} (2n+1) P_n(\cos \alpha) \\ \cos \alpha &= \hat{\mathbf{r}}(\Omega) \cdot \hat{\mathbf{r}}(\Omega') \end{aligned} \quad (3)$$

where  $P_n$  are the un-normalized Legendre polynomials.

Combined with the spherical symmetry of the assumed Earth model (PREM), the axial symmetry of the impulse load (3) allows us to load the  $r$ -layer on the North Pole. In this particular setting,  $\Omega' = 0$ ,  $\alpha = \theta$  and the impulse load (3) is independent of the angular order,  $m$ . The gravity-sensitive poloidal components that are relevant for the tidal problems are (e.g., Melchior, 1978; Longman, 1962)

theory (e.g., Melchior, 1978; Longman, 1962) and consider the static deformation of a self-gravitating elastic mantle shell, i.e.,  $\omega \rightarrow 0$ . The linearized elastogravitational operator for the Green function spectrum

$(U_{nm}, V_{nm}, \Phi_{nm})$  has become classic since Alterman et al. (1959). There are six independent solutions raised by the second order ordinary differential equations on  $(U_{nm}, V_{nm}, \Phi_{nm})$ . When the deformation of the whole earth is considered, three of the six solutions are eliminated inside the inner core as required by regularity at the origin. Since we explicitly treat the mantle as a dynamically independent system passively deforming by the CMB pressure, the elasto-gravitational operator of Alterman et al. (1959) in our case is confined to the spherical mantle shell, starting at the CMB. Therefore, there is no regularity required at the origin of the coordinates, and all six independent solutions have to be incorporated in solving for the Love numbers. Six boundary conditions, three at the CMB,  $b$ , and three at the surface,  $a$ , will be given in detail below to match the six independent solutions.

The elasto-gravitational operator in the mantle shell domain preserves the symmetry properties as in the whole-earth domain. Most noticeably, the operator is independent of the angular order,  $m$ , as a result of spherical symmetry. If the source terms (the loading from outside and within) in the boundary conditions are independent of  $m$  as is the case of our Green functions, then, the radial components in (4) are independent of  $m$ . We have in this situation the degenerate solution  $(U_n, V_n, \Phi_n)$  instead of  $(U_{nm}, V_{nm}, \Phi_{nm})$ . If the source terms in the boundary conditions are  $m$ -dependent, then, the  $m$ -dependent solution  $(U_{nm}, V_{nm}, \Phi_{nm})$  is proportional to a common factor of the source terms. Particularly, if the boundary conditions contain only a single source term, say,  $\psi_{nm}$ , then, the solution can be written as

$$(U_{nm}, V_{nm}, \Phi_{nm}) = \psi_{nm} (U_n, V_n, \Phi_n) \quad (6)$$

where  $(U_n, V_n, \Phi_n)$  is the solution obtained by setting  $\psi_{nm} = 1$ . Analytical (for special cases) and numerical

$$\left( \frac{\partial \Phi_{nm}(r)}{\partial r} \right)_{ex} - \left( \frac{\partial \Phi_{nm}(r)}{\partial r} \right)_{in} = 4\pi G (\rho_{in}(r) - \rho_{ex}(r)) U_{nm}(r) \quad (r = a, b) \quad (7)$$

where  $G$  is the gravitational constant. The subscript *ex* stands for the exterior of the mantle, *in*, the interior of

$$\left( \frac{\partial \Phi_{nm}}{\partial a} \right)_{ex} = -\frac{n+1}{a} \Phi_{nm} \quad \rho_{ex}(a) = 0 \quad \rho_{in}(a) = \rho(a) \quad (8)$$

The exterior of the mantle at the CMB  $b$  is the fluid outer core and the inner core. For harmonic de-

solutions for various problems, mostly in three-solution approaches, have been worked out in numerous publications. An insightful review on the numerical solutions is given by Takeuchi and Saito (1972). The extension from three numerical solutions in the whole earth to six numerical solutions in the mantle shell is trivial. We will not repeat the details of the numerical procedures.

Consider the solution of the Green functions (4) for an impulse force loaded at the CMB at the North Pole. As mentioned earlier, it will result in degenerate solutions  $(U_n, V_n, \Phi_n)$ . Six boundary conditions are needed to accommodate six independent solutions for the elasto-gravitational operator. For a pressure load at the CMB, the outer surface of the elastic Earth is a free surface. Thus, the three boundary conditions, two stress components plus a gravitational potential, are identical to those of the seismic normal mode problems (e.g., Dahlen and Tromp, 1998; Takeuchi and Saito, 1972). We only have to consider three additional boundary conditions at the CMB.

For the stress boundary conditions, we take  $Mg\delta_b$  as the impulse force, instead of a unit impulse force,  $\delta_b$ . Here  $M$  is the total mass of the Earth, and  $g$  the surface gravity  $g \approx 980 \text{ cm/s}^2$ . Although the mantle is dynamically decoupled from the core, they have to be coupled kinematically. This means that the radial displacement  $U_{nm}$  must be continuous across the CMB and in fact any layer of discontinuity in density,  $\rho$ . Without an external mass load, the perturbation in gravitational potential,  $\Phi_{nm}$ , is only due to the deformed mass within the mantle, plus the density contrast at the deflected CMB. The gravitational boundary conditions across the outer surface,  $a$ , and the CMB,  $b$ , are, in a unified form (e.g., Dahlen and Tromp, 1998; Hager and Clayton, 1989; Takeuchi and Saito, 1972)

the mantle. The exterior at the outer surface boundary,  $a$ , is the open air, thus

degrees,  $n \geq 2$ , the center of mass of the cores remains unperturbed in the inertial space by the mantle defor-

mation. Therefore, we can treat the gravitational perturbation in the core as due to the deformed mantle alone for  $n \geq 2$

$$\left(\frac{\partial \Phi_{nm}}{\partial b}\right)_{ex} = \frac{n}{b} \Phi_{nm}, \quad n \geq 2 \quad (9)$$

$$\rho_{ex}(b) = \rho(b^-), \quad \rho_m(b) = \rho(b^+)$$

For degree-1 solution, the center of mass of the cores has to shift a bit in order to maintain the CCMWE fixed in the inertial space. The shift will invalidate this relation (9) (see next section).

Denote by  $T_n^{rr}(r)$  and  $T_n^{r\theta}(r)$  the  $\hat{\mathbf{r}}\hat{\mathbf{r}}$  and  $\hat{\mathbf{r}}\hat{\boldsymbol{\theta}}$  stress components of harmonic degree  $n$ , the complete set of boundary conditions for the Green functions of  $n \geq 2$  is

$$T_n^{rr}(a) = 0 \quad (10a)$$

$$T_n^{r\theta}(a) = 0 \quad (10b)$$

$$\left(\frac{\partial \Phi_n(a)}{\partial a} + 4\pi G \rho(a) U_n(a)\right) + \frac{n+1}{a} \Phi_n(a) = 0 \quad (10c)$$

$$T_n^{rr}(b) = -(2n+1) \frac{Mg}{4\pi b^2} = -(2n+1) \left(\frac{a}{b}\right)^2 \frac{g^2}{4\pi G} \quad (10d)$$

$$T_n^{r\theta}(b) = 0 \quad (10e)$$

$$\left(\frac{\partial \Phi_n(b)}{\partial b} + 4\pi G(\rho(b^+) - \rho(b^-)) U_n(b)\right) - \frac{n}{b} \Phi_n(b) = 0 \quad (10f)$$

The load term in the radial stress component (10d) is the harmonic coefficient of  $Mg\delta_b$  obtained by letting  $Q^l=0$  and  $\alpha=\theta$  in (4). The term  $(a/b)^2$  arises in (10d) by applying the relation  $g=MG/a^2$ .

## DEGREE-1 TERMS FOR THE CMB PRESSURE LOAD

Pressure loads at degree 0 correspond to a pure spherical expansion with no change in surface gravity. We chose to ignore degree zero loads. The peculiarity and sometimes confusion in dealing with the degree-1 terms has to do with a rigid shift solution, arising in the static state  $\omega=0$ . That is, one of the six solutions for the elastio-gravitational operator at degree-1,  $(\tilde{U}_1, \tilde{V}_1, \tilde{\Phi}_1)$ , degenerates into a rigid shift inside the mantle shell  $b \leq r \leq a$

$$\begin{aligned} \tilde{U}_1(r) &= \chi \\ \tilde{V}_1(r) &= \chi \\ \tilde{T}_1^{rr}(r) &= 0 \\ \tilde{T}_1^{r\theta}(r) &= 0 \\ \tilde{\Phi}_1(r) &= -\chi g(r) \\ \frac{\partial \tilde{\Phi}_1(r)}{\partial r} + 4\pi G \rho(r) \tilde{U}_1(r) &= \frac{2\chi}{r} g(r) \end{aligned} \quad (11)$$

where  $g(r)$  is the Earth's gravity as a function of radius, and  $\chi$  represents the amount of the rigid shift. If the whole earth is taken as a self-gravitating elastic medium, as in the classic tidal problems, (11) is also valid in the solid inner core. For the outer core, where the tangential displacement may go to infinity, the rigid shift solution (11) satisfies the Poisson equation (Fang, 1998; Dahlen, 1976; Farrell, 1972).

In order to deal with this rigid shift (11) in a general way, we first recall some basics. A stripped-down mechanical system concerns the balance of three major forces: inertial forces in the form of accelerations, tractions in the form of stresses, and body forces in the form of self and applied gravitation. With properly prescribed initial and boundary conditions, the evolution of the system can be determined uniquely by its governing equations in the form of a local balance of forces. When the inertial forces are dropped by setting  $\omega \rightarrow 0$ , there are only two types of forces balancing each other locally inside the mantle. But the solution (11) is stress free, hence it does not correspond to a balance of forces in the mantle system. The gravity inside the mantle cannot balance itself to give rise to a finite rigid shift. Put in another way, the rigid shift solution (11) at degree 1 allows us to specify the reference frame of the static deformation, but the reference frame cannot be determined by the governing equations in the form of a local balance of forces, because of the missing inertial forces. An additional constraint is required for specifying the reference frame. This constraint, plus the old boundary conditions (10), would make the system overdetermined. The overdetermination can be eased by relaxing the boundary conditions. If the old boundary conditions are consistent with the new constraint, the new constraint is simply redundant. Otherwise, one of the old boundary conditions in (10) has to be discarded to give room for imposing the new constraint. The physical grounds for

such a treatment are the following. The old boundary conditions constrain the state of strains, while the mantle at degree-1 is only partially in a state of strain. Therefore, the old boundary conditions have to be “partially” relaxed to accommodate this partial state of strain. The new constraint in place of the relaxed old boundary condition is used to determine the rigid shift component.

Mathematically, we have six independent solutions of non-zero static strains and six boundary conditions (10a–10f) for degrees  $n \geq 2$ , and the local balance of forces is perfect at each degree. For degree-1, however, we have only five independent solutions for non-zero static strains. One of the six boundary conditions (10) has to be discarded so that a particular solution at degree-1,  $(U_1^p, V_1^p, \Phi_1^p)$ , can be determined by the five independent solutions and five remaining boundary conditions. We notice that the  $(U_1^p, V_1^p, \Phi_1^p)$  so obtained are not unique, because each one of the five solution vectors has six elements in the form of

$$\begin{aligned} \tilde{T}_1^{rr}(a) &= 0 \\ \tilde{T}_1^{r\theta}(a) &= 0 \\ \left( \frac{\partial \tilde{\Phi}_1(a)}{\partial a} + 4\pi G \rho(a) \tilde{U}_1(a) \right) + \frac{2}{a} \tilde{\Phi}_1(a) &= 0 \\ \tilde{T}_1^{rr}(b) &= 0 \\ \tilde{T}_1^{r\theta}(b) &= 0 \\ \left( \frac{\partial \tilde{\Phi}_1(b)}{\partial b} + 4\pi G (\rho(b^+) - \rho(b^-)) \tilde{U}_1(b) \right) - \frac{1}{b} \tilde{\Phi}_1(b) &= 3 \frac{g(b)}{b} - 4\pi G \rho(b^-) \end{aligned} \quad (13)$$

It is clear that the first five boundary conditions in (13) are homogeneous to the rigid shift solution. Thus, the five boundary conditions would not be violated by the final solution (12), if and only if the first five (10a–10e) are chosen for computing the particular solution  $(U_1^p, V_1^p, \Phi_1^p)$ . The boundary condition that has to be discarded from (10) for degree-1 is (10f). The physical justification of this decision can be seen shortly.

The next step is to determine the amount of shift,  $\chi$ , by incorporating an additional constraint. We place the origin of our reference frame at the combined center of mass of the mantle and the core i.e., the

$$\Phi_1^{core}(r) = -\frac{4\pi G b^3 (\rho(b^-) - \rho(b^+))}{3r^2} (U_1^p(b) + \chi) \quad r > b \quad (15)$$

It follows from (12), (14), and (15) that

the left hand side of (11), while we have only five boundary conditions available. One can easily prove that if the five boundary conditions chosen are homogeneous (identically zero) to the rigid shift solution (11), then the non-unique particular solutions  $(U_1^p, V_1^p, \Phi_1^p)$  differ with each other only by a rigid shift. The amount of shift,  $\chi$ , is determined by incorporating an additional constraint usually associated with the center of mass. The complete solution at degree-1 is reached by adding the components of the rigid shift (11) to the particular solution  $(U_1^p, V_1^p, \Phi_1^p)$

$$\begin{aligned} U_1(r) &= U_1^p(r) + \chi \\ V_1(r) &= V_1^p(r) + \chi \\ \Phi_1(r) &= \Phi_1^p(r) - \chi g(r) \end{aligned} \quad (12)$$

To see which one of the six boundary conditions must be discarded, we substitute (11) into the left hand side of (10a–10f) to obtain

CCMWE. The total potential of the mantle and the core must vanish at degree-1 outside the surface of the Earth

$$(\Phi_1^p(a) - \chi g(a)) + \Phi_1^{core}(a) = 0 \quad (14)$$

where  $\Phi_1^{core}(r)$  is the degree-1 coefficient of the potential perturbation from the core. Neglecting the density anomaly inside the core, we already assume that  $\Phi_1^{core}(r)$  is generated only by the deflection at the boundary of the outer core of density  $\rho(b^-)$ , which is welded to the deformed lower boundary of the mantle of density  $\rho(b^+)$ .

$$\chi = \frac{\Phi_1^p(a) - \frac{4\pi G b^3 (\rho(b^-) - \rho(b^+))}{3a^2} U_1^p(b)}{g(a) + \frac{4\pi G b^3 (\rho(b^-) - \rho(b^+))}{3a^2}} \quad (16)$$

The physical justification for discarding the boundary condition (10f) manifests itself through our discussions from (14) to (16). In fact, the boundary condition (10f) represents a physical state where the perturbation in gravitational potential within the core is due to the deformed mantle only. This is not true at degree-1: the center of mass of the deformed mantle shifts in the inertial space, and the center of mass of the core has to shift accordingly to maintain the stationary CCMWE. As a result, the potential perturbation within the core is a combined effect of the deformed mantle and shifted center of mass of the cores. If the entire core is an incompressible fluid of constant density, there may not be degree-1 pressure exerted at the CMB, because the boundary condition (10f) must be valid at degree-1.

Our analysis from (11) to (16) is independent of a particular set of the five boundary conditions (10a–10e). In other words, the shift obtained by (16) also applies to the problem of a Mass-Related-Surface-Pressure (MRSP) load on a mantle shell with or without a dynamically decoupled core. Although this MRSP loading on a mantle shell has little value in practice, it proves to be a good thought-experiment in helping understand the connection between our treatment of the degree-1 terms and the treatment of Farrell (1972) and Dahlen (1976). Suppose we consider an identical MRSP load as Longman's (1962) on a mantle shell in the presence of a dynamically decoupled fluid core. The three homogeneous surface boundary conditions (10a–10c) then become inhomogeneous.

$$T_1^{rr}(a) = -\frac{3g^2}{4\pi G} \quad (17a)$$

$$T_1^{r\theta}(a) = 0 \quad (17b)$$

$$\left( \frac{\partial \Phi_1(a)}{\partial a} + 4\pi G \rho(a) U_1(a) \right) + \frac{2}{a} \Phi_1(a) = -3g \quad (17c)$$

The CMB becomes a purely free-slip boundary without pressure load (e.g., Hager and Clayton, 1989).

Repeating the analysis from (11) through (16), we obtain the degree-1 shift  $\chi$ . Now let us shrink the volume of the core by  $b \rightarrow 0$ , the free-slip boundary conditions at the CMB will then be replaced by the regularity condition at the origin,  $U_1(0) = V_1(0) = \Phi_1(0) = 0$ . Hence, the problem reduces to the exact Longman's (1962) MRSP load problem on a coreless solid earth. In the mean time, we have from (16)

$$\lim_{b \rightarrow 0} \chi = \frac{\Phi_1^p(a)}{g(a)} \quad (18)$$

This is exactly the same degree-1 shift derived by Farrell (1972) and Dahlen (1976) for the MRSP load problem. We can see at this point that the treatments by Farrell (1972) and Dahlen (1976) on the degree-1 terms is just a special case of the general procedure introduced here.

What is remarkable about the degree-1 terms in the MRSP load problem is that the three surface boundary conditions are self-consistent through the compatibility relation (Saito, 1974; Farrell, 1972)

If the particular solution ( $U_1^p$ ,  $V_1^p$ ,  $\Phi_1^p$ ) in this MRSP problem is determined by any two of the three boundary conditions in (17), the third (discarded) boundary condition is met automatically by ( $U_1^p$ ,  $V_1^p$ ,  $\Phi_1^p$ ) through the compatibility relation (19). Physically, this degree-1 self-consistence in boundary conditions for MRSP loading results from the fact that the Earth as a whole adjusts to the external loading to keep the CCMWE stationary in space. In contrast, for the CMB pressure loading, the mantle and the core have to adjust each other internally to cancel out the degree-1 hemispherical asymmetry in gravitational potential to keep the CCMWE stationary in space. The boundary condition (10f) that gravitationally couples the deformed mantle and the core is incompatible to the non-deformational rigid shift adjustment at degree-1, and hence must be replaced by the CCMWE condition (14).

$$T_1^{rr}(a) + 2T_1^{r\theta}(a) - \frac{g}{4\pi G} \left( \frac{\partial \Phi_1(a)}{\partial a} + 4\pi G \rho(a) U_1(a) \right) + \frac{2}{a} \Phi_1(a) = 0 \quad (19)$$

### NEW DEFINITION FOR CMB PRESSURE LOAD LOVE NUMBERS

To make the load Love numbers comparable with

$$U_n(a) = \left(\frac{a}{b}\right)^2 ah_n \quad V_n(a) = \left(\frac{a}{b}\right)^2 al_n \quad \Phi_n(a) = -\left(\frac{a}{b}\right)^2 k_n ag \quad (20)$$

The minus sign incurred in the  $k_n$  equation in (20) is because we adopt the physical convention for the potential which is opposite in sign with the geodetic convention (e.g., Heiskanen and Moritz, 1968).

$$\begin{aligned} {}_b\mathbf{U}(a, \Omega, \Omega') &= \left(\frac{a}{b}\right)^2 \frac{a}{Mg} \sum_{n=0}^{\infty} \left( \hat{\mathbf{r}} h_n P_n(\cos \alpha) + \hat{\theta} l_n \frac{\partial}{\partial \alpha} P_n(\cos \alpha) \right) \\ {}_b\Phi(a, \Omega, \Omega') &= -\left(\frac{a}{b}\right)^2 \frac{a}{M} \sum_{n=0}^{\infty} k_n P_n(\cos \alpha) \end{aligned} \quad (21)$$

Here we return the variable from  $\theta$  back to  $\alpha$ . Advantages of this new definition of the CMB pressure load Love numbers (20) can be seen by computing the perturbed fields (1) with an arbitrary CMB pressure  $p(\Omega)$ . The CMB pressure,  $p(\Omega)$ , can be represented by its spectrum,  $p_{nm}$ , with the normalized harmonics  $\bar{Y}_{nm}(\theta, \varphi)$

$$p(\Omega) = \sum_{n=0}^{\infty} \sum_{m=-n}^n p_{nm} \bar{Y}_{nm}(\theta, \varphi) \quad (22)$$

Our normalization for the harmonics  $\bar{Y}_{nm}(\theta, \varphi)$  is consistent with Heiskanen and Moritz (1968) and Stacey (1991). Substituting (21) and (22) into (1) and using the addition theorem for spherical harmonics, we obtain the radial component,  $u_r$ , of the displacement and the potential perturbation,  $\phi$

$$\begin{aligned} u_r(a, \Omega) &= \frac{3}{\rho_E g} \sum_{n=0}^{\infty} \frac{h_n}{2n+1} \sum_{m=-n}^n p_{nm} \bar{Y}_{nm}(\Omega) \\ \phi(a, \Omega) &= -\frac{3}{\rho_E} \sum_{n=0}^{\infty} \frac{k_n}{2n+1} \sum_{m=-n}^n p_{nm} \bar{Y}_{nm}(\Omega) \end{aligned} \quad (23)$$

where  $\rho_E$  is the average density of the Earth. Relations in (23) are identical to those for the MRSP loads, except that for the MRSP loads, we usually have  $(1+k_n)$  instead of the single number  $k_n$  in the  $\phi$  equation, because the mass load itself contributes to the potential perturbation. As far as the load Love numbers,  $k_n$ ,

the classical SMRP load Love numbers, we redefine the load Love numbers  $h_n, l_n, k_n$  for the CMB pressure load based on the Green functions for the  $Mg\delta_b$  load

The harmonic spectrum for the Green functions for the unit impulse force  $\delta_b$  are recovered by dividing (18) by  $1/Mg$ . The complete expressions for the Green functions are

they only correspond to the potentials generated by the deformed Earth's perturbed density. Therefore, the load Love numbers defined by (20) for the motion-related CMB pressure loads are completely comparable with the load Love numbers for the MRSP loads.

### RESULTS AND DISCUSSIONS

Table 1 lists the load Love numbers calculated for the CMB pressure up to degree-10. A striking feature in the list is a large negative degree-1 vertical Love number,  $h_1$ , standing out among the otherwise all-positive  $h_n$  ( $n \geq 2$ ). The positive  $h_n$  ( $n \geq 2$ ) is consistent with intuition: a positive pressure at the CMB

**Table 1 Load Love numbers for the CMB pressure load**

$n$	$h_n$	$l_n$	$k_n$
1	-1.425 23	-0.434 03	0.227 76
2	0.658 98	-0.023 60	0.317 35
3	0.352 21	-0.052 79	0.109 24
4	0.194 33	-0.031 93	0.043 81
5	0.113 13	-0.017 76	0.019 90
6	0.067 97	-0.009 84	0.009 76
7	0.041 35	-0.005 47	0.005 00
8	0.025 19	-0.003 04	0.002 63
9	0.015 30	-0.001 69	0.001 40
10	0.009 24	-0.000 94	0.000 75



pushes the mantle up from below to cause positive vertical displacement.

This negative  $h_1$  is markedly different from the MRSP loading, where the degree-1,  $h_1'$  (prime is used to distinguish the MRSP loading), is of the same sign with the higher degrees  $h_n'$ ,  $n \geq 2$ . The phenomenological cause of the negative  $h_1$  is shown schematically in Fig. 1. In the undeformed state, the center of mass of the mantle and the center of mass of the core coincide with the CCMWE at position, say, O (Fig. 1a). When an impulse pressure load is applied at the North Pole in the positive direction, the degree-1 component of strained-deformation produces thickening above the point of load and thinning at its antipodal point within the mantle. This asymmetric thickening-thinning shifts

the center of mass of the mantle towards the North Pole. The shifted center of mass of the mantle in turn brings the center of mass of the inner core upwards by gravitational attraction. The shifts of center of masses of the mantle and inner core are offset by the downward shift of the fluid outer core. The downward shift in the center of mass of the fluid outer core is not strong enough to offset the shift in the center of mass of the mantle in inertial space. As a result, the whole Earth undergoes a rigid shift towards the South Pole in inertial space to keep the CCMWE stationary (Fig. 1a). The mantle thickening at the point of load and the upward shift of the inner core bring extra mantle mass closer to the point. This is why the gravitational  $k_1$  is positive ( $k_1 > 0$ ).

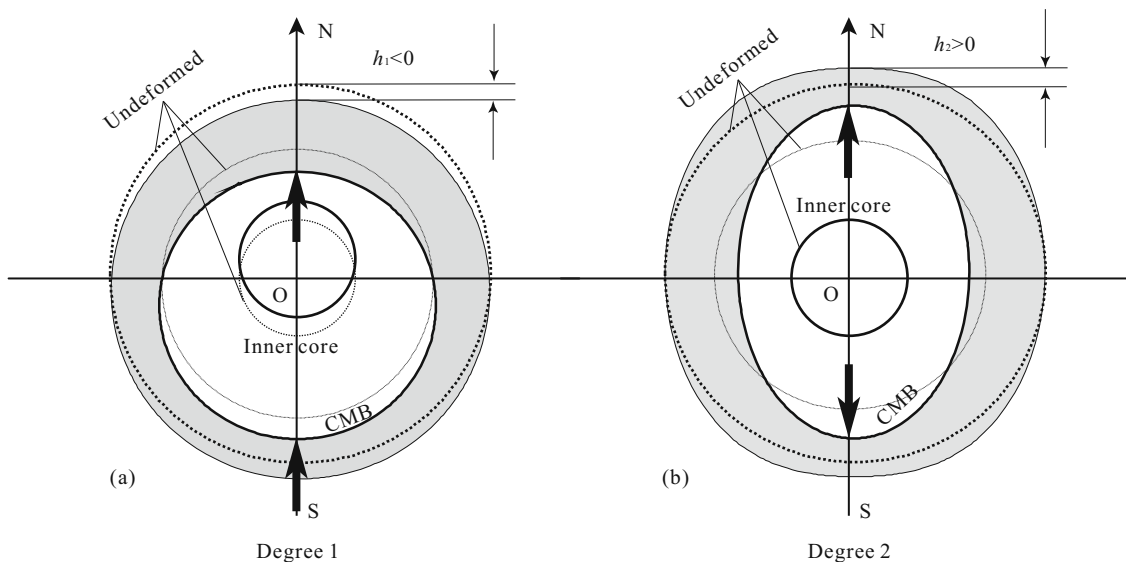


**Figure 1. Schematic displacements at degrees 1 and 2 for an impulse load on the North Pole at the CMB in reference to the undeformed surface and CMB in inertial space. The CCMWE is located at the point O. Arrows indicate the directions of the pressure load at the North and South poles. Concentric dashed lines indicate the undeformed inner core boundary, CMB and the surface.**

The kinematic explanation does not address the question why at degree-1 the mantle is thickened at the North Pole (Fig. 2). For the directions of forcing in Fig. 1a, the North Pole is expected to be thinned, with the thickening taking place at the South-Pole. A full explanation of this unusual thickening at the North Pole requires additional testing. Detailed analyses and testing are conducted in a separate paper.

Another interesting feature revealed in our calculations is the non-integer  $k_1$ . In the case of the MRSP loads,  $k_1'$  is known as  $k_1' = 0$ , if the reference

frame is centered at the center of mass of the deformed earth (Dahlen, 1976; Farrell, 1972). Or we have  $k_1' = -1$ , if the origin of the reference frame is placed at the CCMWE (Conrad and Hager, 1997). In the case of a CMB pressure load, we find  $k_1 = 0.22776$  by placing the origin of the reference frame at the CCMWE. This non-integer  $k_1$  measures the potential perturbation in the deformed mantle to balance the potential perturbation of the deformed core in order to keep the CCMWE fixed in inertial space. This non-integer  $k_1$  of the deformed mantle cannot be re-

lated to gravitational observations at the surface especially when the gravity is derived from satellite ranging. As far as the solid earth, geodetic techniques are only sensitive to the CCMWE. However, this non-integer  $k_1$  is important for studying the interaction between the core and the mantle, which will be considered elsewhere.

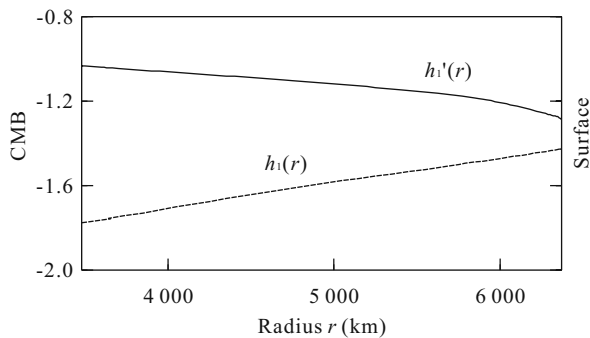


**Figure 2. Degree-1 vertical Love numbers for the CMB pressure load (dashed line) and the MRSP load (solid line) as functions of radius within the mantle. Note, the surface value for the MRSP Love number  $h_n'(a)=-1.29$ , because the reference frame is centered at the CCMWE.**

The comparison between the SMRP loading and the CMB pressure loading for  $n>1$  is shown in Fig. 3, where the surface mass load Love numbers,  $h_n'$  and  $k_n'$  are calculated based on the procedure in Fang (1998). As shown in Fig. 3, the rapid decrease of the CMB  $h_n$ , as a function of  $n$ , is due to the great depth of the CMB. Specifically, the convergence connects to the issue of penetration depth. A well known property of the elasto-gravitational operator of Alterman et al. (1959) is that, when the Earth undergoes a free oscillation, or the source of excitation is near the Earth's surface, the radial perturbations ( $U_n(r)$ ,  $V_n(r)$ ,  $\Phi_n(r)$ ) penetrate down from the surface as a function of degree  $n$ . The higher the degree, the shallower the radial perturbations penetrate. This is the foundation for the equivalence of high degree seismic normal modes and surface waves (e.g., Dahlen and Tromp, 1998; Aki and Richards, 1980; Takeuchi and Saito, 1972). Fang and Hager (1999) have made a quantitative analysis on the penetration depth for the MRSP load Love numbers,  $h_n'$ . For the CMB pressure loads, the radial perturbations ( $U_n(r)$ ,  $V_n(r)$ ,  $\Phi_n(r)$ ) penetrate the mantle upwards from the CMB. The vertical  $h_n$  penetrates

through the mantle only up to degree-6. One reason for such a rapid decrease is that the perturbations spreads from the CMB outwards to a broader space, like a wave from a point source. The outward spreading reduces the deformation energy at locations farther away from the source more rapidly than the inward propagation of perturbations from the surface.

The MRSP load,  $h_n'$ , does not converge to zero. As  $n \rightarrow \infty$ ,  $h_n'$  converges to a number in the range of  $-10$ – $-3$ . The reason we do not specify the limit  $h_\infty'$  is that for ultra high degrees, the penetration depths of  $h_n'$  are extremely shallow, and the value of  $h_n'$  are critically sensitive to the crustal structure. The crust is very heterogeneous in the transverse direction, it is meaningless to consider  $h_\infty'$  for a model with a spherically symmetric thin crust.

The most intriguing revelation in the calculations in Table 1 and the plots in Fig. 3 is that the gravitational  $k_n$  for the motion-related CMB pressure loads are nearly identical in absolute value with their counterparts  $k_n'$  for the MRSP loads. This means that if the projections of pressure fields from the surface and the CMB onto the surface of a unit sphere are identical, the deformed mantle mass will produce nearly identical potential perturbations at the Earth's surface, only opposite in sign, for both pressure loads, regardless of the depth of the CMB pressure. To understand this important feature, we first notice from Fig. 2 that the vertical  $h_n'$  curve is markedly different from the gravitational  $k_n'$  curve. The diverging  $h_n'$  (in Fig. 3) represents a significant surface deformation caused by the surface load. The rapidly converging (to zero)  $k_n'$  curve implies a rapid decrease of deformation in the Earth's interior i.e. a decrease in penetration depth. In other words, a surface pressure load produces a significant deformation at the surface but much less significant deformation in the interior. The CMB pressure produces much less significant deformation at the surface, as it should, but significant deformation in the interior, because the interior is closer to the source of load. This relatively significant deformation in the interior contributes most for the gravitational  $k_n$ .

Finally, for geodetic signatures from the core motion, it is more important to examine the individual harmonic coefficients than to calculate the global patterns, using (23). There are continuing efforts in the

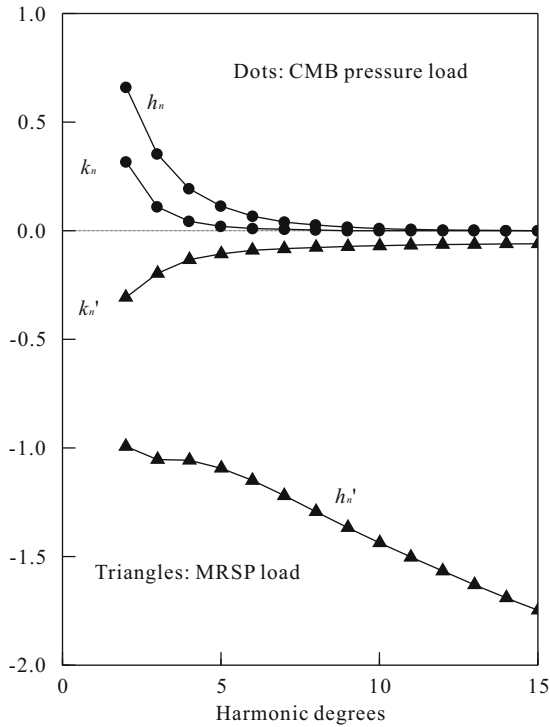


**Figure 3. Love numbers, starting from degree-2, for the CMB pressure load,  $h_n$  and  $k_n$  versus the Love numbers for the mass-related surface pressure (MRSP) load,  $h_n'$  and  $k_n'$ . Details for the calculations are in the text.**

determination and geophysical interpretation of the time variation of the Earth’s gravity field in the degree-2 zonal coefficient, known as  $J_2$  dot (e.g., Cheng and Tapley, 2004; Cox and Chao, 2002; Dickey et al., 2002; Cheng et al., 1997). The incremental  $\delta J_2$  caused by the mass-related surface pressure  $p'$  is

$$\delta J_2 = -\frac{3}{a\rho_E g\sqrt{5}}(1+k'_2)p'_{20} \tag{24}$$

where  $p'_{20}$  is the degree-2 and order 0 coefficient in the harmonic expansion (20) for the pressure  $p'$ , and  $k'_2 \approx -0.31$ . The incremental  $\delta J_2$  caused by the CMB pressure load is

$$\delta J_2 = -\frac{3k_2}{a\rho_E g\sqrt{5}}p_{20} \tag{25}$$

Suppose  $p'_{20} = p_{20}$ , then we have, from (24) and (25)

$$\frac{\delta J_2(\text{CMB})}{\delta J_2(\text{surface})} \approx 0.5 \tag{26}$$

Relation (26) states that the  $J_2$  perturbation from the CMB pressure is about half the value of the  $J_2$  perturbation from the mass-related surface pressure if the

coefficients,  $p_{20}$ , are identical. We may also find from (26) that

$$\delta J_2(\text{CMB}) \approx -1.3 \times 10^{-10} p_{20}/\text{hpa} \tag{27}$$

**ACKNOWLEDGMENT**

We thank Drs. David A Yuen, Vernon F Cormier, and Sidao Ni for organizing this stimulating workshop; and Dr. Vernon F Cormier for careful and constructive review.

**REFERENCES CITED**

Aki, K., Richards, P. G., 1980. Quantitative Seismology. University Sci. Book, Sausalito, CA

Alterman, Z., Jarrosh, H., Pekeris, C. L., 1959. Oscillation of the Earth. *Proc. R. Soc. Lond. A.*, 252(1268): 80–95

Buffett, B. A., 1996. Gravitational Oscillations in the Length of Day. *Geophys. Res. Lett.*, 23(17): 2279–2282

Cheng, M. K., Shum, C. K., Tapley, B. D., 1997. Determination of Long-Term Changes in the Earth’s Gravity Field from Satellite Laser Ranging Observations. *J. Geophys. Res.*, 102(B10): 22377–22390

Cheng, M. K., Tapley, B. D., 2004. Variations in the Earth’s Oblateness during the Past 28 Years. *J. Geophys. Res.*, 109(B9): B09402, doi:10.1029/2004JB003028

Conrad, C. P., Hager, B. H., 1997. Spatial Variation in the Rate of Sea Level Rise Caused by the Present-Day Melting of Glaciers and Ice Sheets. *Geophys. Res. Lett.*, 24(12): 1503–1506

Cox, C. M., Chao, B. F., 2002. Detection of a Large-Scale Mass Redistribution in the Terrestrial System since 1998. *Science*, 297(5582): 831–833

Dahlen, F. A., 1976. The Passive Influence of the Oceans upon the Rotation of the Earth. *Geophys. J. R. Astron. Soc.*, 46(2): 363–406

Dahlen, F. A., Tromp, J., 1998. Theoretical Global Seismology. Princeton Uni. Press, Princeton

Dickey, J. O., Marcus, S. L., de Viron, O., et al., 2002. Recent Earth Oblateness Variations: Unraveling Climate and Postglacial Rebound Effects. *Science*, 298(5600): 1975–1977

Dumberry, M., Bloxham, J., 2004. Variation in Earth’s Gravity Field Caused by Torsional Oscillation in the Core. *Geophys. J. Int.*, 159(2): 417–434

Dziewonski, A. M., Anderson, D. L., 1981. Preliminary Reference Earth Model. *Phys. Earth Planet. Int.*, 25(4):

297–356

- Fang, M., 1998. Static Deformation of the Outer Core. In: Wu, P., ed., *Dynamics of the Ice Age Earth*. Georesearch Forum. *Trans. Tech. Pub. Switzerland*, 3–4: 155–190
- Fang, M., Hager, B. H., 2001. Vertical Deformation and Absolute Gravity. *Geophys. J. Int.*, 146: 539–548
- Fang, M., Hager, B. H., Herring, T. A., 1996. Surface Deformation Caused by Pressure Changes in the Fluid Core. *Geophys. Res. Lett.*, 23(12): 1493–1496
- Farrell, W. E., 1972. Deformation of the Earth by Surface Loads. *Rev. Geophys. & Space Phys.*, 10(3): 761–797
- Gire, C., Le Mouél, J. L., 1990. Tangentially Geostrophic Flow at Three Core-Mantle Boundary Compatible with the Observed Geomagnetic Secular Variation: The Large Scale Component of the Flow. *Phys. Earth Planet. Inter.*, 59(4): 259–287
- Glatzmaier, G. A., Roberts, P. H., 1995. A Three-Dimensional Self-Consistent Computer Simulation of a Geomagnetic Field Reversal. *Phys. Earth Planet. Inter.*, 91(1–3): 63–75
- Greff, M. P., LeMouél, J. L., 2004. Surface Gravitational Field and Topography Changes Induced by the Earth's Fluid Core Motions. *J. Geodesy*, 78: 386–392
- Gubbins, D., Sreenivasan, B., Mound, J., et al., 2011. Melting of the Earth's Inner Core. *Nature*, 473: 361–363, doi:10.1038/nature10068
- Hager, B. H., Clayton, R. W., 1989. Constraints on the Structure of Mantle Convection Using Seismic Observation, Flow Model, and the Geoid. In: Peltier, R. W., ed., *Mantle Convection*. Gordon & Breach, New York
- Heiskanen, W. A., Moritz, H., 1968. *Physical Geodesy*. Freeman & Company, New York
- Irving, J. C. E., Deuss, A., Woodhouse, J. H., 2009. Normal Mode Coupling due to Hemispherical Anisotropic Structure in Earth's Inner Core. *Geophys. J. Int.*, 178(2): 962–975
- Jackson, A., Bloxham, J., Gubbins, D., 1993. Time-Dependent Flow at the Core Surface and Conservation of Angular Momentum in the Coupled Core-Mantle System. In: LeMouél, J. L., Smylie, D. E., Herring, T., eds., *Dynamics of the Earth's Deep Interior and Earth Rotation*. *AGU Geophysical Monograph*, 72: 97–107
- Kuang, W., Bloxham, J., 1997. A Numerical Model of the Generation of the Earth's Magnetic Field. *Nature*, 365: 371–374
- Longman, I. M., 1962. A Green's Function for Determining the Deformation of the Earth under Surface Mass Loads, 1, Theory. *J. Geophys. Res.*, 67(2): 845–850
- Melchior, P., 1978. *The Tide of the Planet Earth*. Pergamon Press, Oxford
- Monnereau, M., Calvet, M., Margerin, L., 2010. Lopsided Growth of Earth's Inner Core. *Science*, 328(5981): 1014–1017, doi:10.1126/science.1186212
- Niu, F., Wen, L., 2001. Hemispherical Variations in Seismic Velocity at the Top of the Earth's Inner Core. *Nature*, 410: 1081–1084
- Olson, P., Deguen, R., 2012. Eccentricity of the Geomagnetic Dipole Caused by Lopsided Inner Core Growth. *Nature*, 5: 565–569, doi:10.1038/NGEO1506
- Roberts, P. H., Scott, S., 1965. On Analysis of Secular Variation, 1, A Hydromagnetic Constraint. *J. Geomagn. Geoelectr.*, 17: 137–151
- Saito, M., 1974. Some Problems of Static Deformation of the Earth. *J. Phys. Earth.*, 22: 123–140
- Stacey, F. D., 1991. *Physics of the Earth*. 3rd ed.. Wiley, New York
- Takeuchi, H., Saito, M., 1972. *Seismic Surface Waves in the Computational Physics*. Acad. Press, New York. 217–295
- Taylor, J. B., 1963. The Magneto-Hydrodynamics of a Rotating Fluid and the Earth's Dynamo Problem. *Proc. R. Soc. Lond. A.*, 274(1357): 274–283
- Vamos, C., Suci, N., 2011. Seismic Hemispheric Asymmetry Induced by Earth's Inner Core Decentering. arXiv preprint arXiv:1111.1121
- Wahr, J., de Vries, D., 1989. The Possibility of Lateral Structure inside the Core and Its Implications for Nutation and Earth Tide Observations. *Geophys. J. Int.*, 99(3): 511–519

#### APPENDIX: FORMAL CONSIDERATION OF THE ELASTIC SHELL MODEL

Distinction between external and internal forcing in the surface loading is a delicate issue in geodynamics. Here we conduct a formal analysis to validate the spherical shell simplification for the CMB pressure loading.

Denote by  $a$ ,  $b$ , and  $c$ , respectively, the radii of the Earth surface, the CMB, and the inner-outer core boundaries in an undeformed equilibrium state. Superscripts of  $a$ ,  $b$ , and  $c$  represent the physical variables within the mantle, outer-core and the inner-core. Subscript 0 is used to denote the initial state. Since the CMB pressure variation is generated by the core dynamics, the complete treatment of the problem is to solve the coupled system simultaneously under different regimes. In the form of operators, we may write the governing equations as

$$\begin{aligned}
\mathcal{E}(\mathbf{u}^a, \rho^a, \Phi^a, \mathbf{g}^a) &= 0 \\
\mathcal{H}(\mathbf{u}^b, \mathbf{V}^b, \rho^b, \Phi^b, \mathbf{g}^b, T^b, \mathbf{B}^b, p^b) &= 0 \\
\mathcal{T}(\mathbf{u}^c, \rho^c, \Phi^c, \mathbf{g}^c, T^c, \mathbf{B}^c) &= 0
\end{aligned} \tag{A-1}$$

Here the operator  $\mathcal{E}$  represents an elastic regime governing the displacement,  $\mathbf{u}$ , density,  $\rho$ , potential  $\Phi$ , and the gravity  $\mathbf{g}$ .  $\mathcal{H}$  is the magnetohydrodynamic (MHD) operator that governs the displacement,  $\mathbf{u}$ , velocity  $\mathbf{V}$ , density,  $\rho$ , potential  $\Phi$ , gravity  $\mathbf{g}$ , temperature  $T$ , magnetic field  $\mathbf{B}$ , and the pressure field  $p$ . The last operator,  $\mathcal{T}$ , represents the regime of thermal-magneto-elasticity, governing the variables,  $\mathbf{u}$ ,  $\rho$ ,  $\Phi$ ,  $\mathbf{g}$ ,  $T$ , and  $\mathbf{B}$ .

The variables in (A-1) should be understood as deviations from the reference state. For example, we may choose the reference state to be the Taylor state, in which the Lorentz axial torques on the surfaces of cylinders co-axial with the rotational axis and across the outer core (called the Taylor cylinders) vanish (Taylor, 1963). The flow field in this state does not include any torsional oscillation. A small departure from the reference state, i.e. the small Lorentz torques on the Taylor cylinders are balanced by fluid inertia, thus driving torsional oscillation. The operator  $\mathcal{H}$  therefore includes this torsional oscillation generation mechanism. For simplicity, let us assume that  $\mathcal{H}$  is indeed the operator for the torsional oscillation on the part of the flow field  $\mathbf{V}^b$ . The ultimate forcing, for maintaining the reference state and for driving the torsional oscillation (i.e., to maintain a finite magnetic field in the core), is presumably the thermal-compositional buoyancy force.

If there are no significant material exchange and phase

$$\begin{aligned}
\mathbf{u}^a(\tilde{b}+0) &= \mathbf{u}^b(\tilde{b}-0) \\
\Phi^a(\tilde{b}+0) &= \Phi^b(\tilde{b}-0) \\
\partial_r \Phi^a(b+0) + 4\pi G \rho^a(b+0)u_r(b) &= \partial_r \Phi^b(b-0) + 4\pi G \rho^b(b+0)u_r(b)
\end{aligned} \tag{A-4}$$

The boundary conditions at the outer surface are

$$\begin{aligned}
\Gamma_{rr}^a(\tilde{a}) &= 0 \\
\Gamma_{r\theta}^a(\tilde{a}) &= 0 \\
\partial_r \Phi^a(\tilde{a}-0) + 4\pi G \rho^a(\tilde{a}-0)u_r(a) &= \partial_r \Phi^a(a+0)
\end{aligned} \tag{A-5}$$

Note the last one in (A-4) is not built on the deformed boundary. This is because we need to have a ‘‘surface density’’ for gravity across a 2D boundary. The surface density is formed by a thin layer of thickness,  $u_r(b)$ , as  $(\rho^a(b+0) - \rho^b(b-0))u_r(b)$ .

It is evident from mathematical consideration, that if and only if the CMB pressure,  $p^b(\tilde{b}-0)$  in (A-3) is prescribed by

$$\Gamma_{rr}^a(\tilde{a}) = 0 \tag{A-6a}$$

$$\Gamma_{r\theta}^a(\tilde{a}) = 0 \tag{A-6b}$$

$$\partial_r \Phi^a(\tilde{a}-0) + 4\pi G \rho^a(\tilde{a}-0)u_r(a) = \partial_r \Phi^a(a+0) \tag{A-6c}$$

changes among the Earth’s three major layers in time scales of interests, the system (A-1) is coupled in two ways: One is through self-gravitation, the second way in which the system is coupled is through the boundary conditions on the deformed boundaries.

Even though the forcing of the geodynamo motion in the core remains obscured, it is mostly likely that thermal and compositional forcing dominate the balance of energy leakage, at least we assume so. As an implication of this assumption, density anomaly in the core is predominantly of thermal and compositional origin, and perturbations from mantle gravity on the core density plays a minor role. In other words, gravitational coupling between the core and mantle could be neglected in the geodynamo motion. Then there is only one way the system is coupled, that is through boundary conditions.

We use the over-tilde to distinguish the deformed boundaries from the undeformed. For a viscous boundary layer, co-rotating with the mantle at the upper reach of the outer core, we have the boundary condition

$$\mathbf{V}^b(\tilde{b}-0) = 0 \tag{A-2}$$

On the mantle side, the radial component of the stress tensor  $\Gamma_{rr}^a$  (the notation for stress is different from in the text) balances the pressure from the outer core

$$\Gamma_{rr}^a(\tilde{b}+0) = -p^b(\tilde{b}-0) \tag{A-3}$$

The remaining boundary conditions at the CMB relevant for our discussion are

‘‘observations’’, then, the boundary conditions in (A-3), (A-4) and (A-5) become self-sufficient for the elastic regime  $\mathcal{E}$ . Thus, the mantle deformation can be determined, without regarding details of the motion in the core, by the six equations adopted in the text and six essential boundary conditions stripped-down from (A-3), (A-4), and (A-5)

$$\Gamma_r^b(\tilde{b}) = -p^b(\tilde{b} - 0) \quad (\text{A-6d})$$

$$\Gamma_{r\theta}^a(\tilde{b}) = 0 \quad (\text{A-6e})$$

$$\partial_r \Phi^a(b+0) + 4\pi G \rho^a(b+0)u_r(b) = \partial_r \Phi^b(b-0) + 4\pi G \rho^b(b+0)u_r(b) \quad (\text{A-6f})$$

These are essentially the same boundary conditions as in (10), except that some of them in are on the deformed boundaries while in (10) the boundary conditions seem to be on the

undeformed boundaries. This technical discrepancy can be resolved by the equivalence between Lagrangian and Eulerian in the linear theory for infinitesimal deformation.